

## DETERMINATION OF LAYER-CHARGE CHARACTERISTICS OF SMECTITES

G. E. CHRISTIDIS<sup>1,\*</sup> AND D. D. EBERL<sup>2</sup>

<sup>1</sup> Technical University of Crete, Department of Mineral Resources Engineering, 73100 Chania, Greece

<sup>2</sup> US Geological Survey, 3215 Marine St., Suite E-127, Boulder, Colorado 80303-1066, USA

**Abstract**—A new method for calculation of layer charge and charge distribution of smectites is proposed. The method is based on comparisons between X-ray diffraction (XRD) patterns of K-saturated, ethylene glycol-solvated, oriented samples and calculated XRD patterns for three-component, mixed-layer systems. For the calculated patterns it is assumed that the measured patterns can be modeled as random interstratifications of fully expanding 17.1 Å layers, partially expanding 13.5 Å layers and non-expanding 9.98 Å layers. The technique was tested using 29 well characterized smectites. According to their XRD patterns, smectites were classified as group 1 (low-charge smectites) and group 2 (high-charge smectites). The boundary between the two groups is at a layer charge of  $-0.46$  equivalents per half unit-cell. Low-charge smectites are dominated by 17.1 Å layers, whereas high-charge smectites contain only 20% fully expandable layers on average. Smectite properties and industrial applications may be dictated by the proportion of 17.1 Å layers present. Non-expanding layers may control the behavior of smectites during weathering, facilitating the formation of illite layers after subsequent cycles of wetting and drying. The precision of the method is better than 3.5% at a layer charge of  $-0.50$ ; therefore the method should be useful for basic research and for industrial purposes.

**Key Words**—Charge Distribution, Expandable Layers, K-saturation, Layer Charge, LayerCharge Program, Profile Modeling, Smectite, X-ray Diffraction.

### INTRODUCTION

Characterization of smectite layer charge is of economic and geologic importance, because layer charge strongly affects key smectite properties such as swelling (e.g. MacEwan and Wilson, 1980; Güven, 1988), cation exchange capacity (CEC), and ion exchange selectivity (e.g. Maes and Cremers, 1977). Smectites are often compositionally and structurally heterogeneous (e.g. Tettenhorst and Johns, 1966; Stul and Mortier, 1974; Lagaly and Weiss, 1975; Talibudeen and Goulding, 1983; Nadeau *et al.*, 1985; Lim and Jackson, 1986; Decarreau *et al.*, 1987; Goodman *et al.*, 1988; Iwasaki and Watanabe, 1988; Lagaly, 1994; Christidis and Dunham, 1993, 1997). This heterogeneity contributes significantly to layer-charge heterogeneity, both in terms of charge location (tetrahedral or beidellitic vs. octahedral or montmorillonitic charge) and charge magnitude (i.e. individual smectite 2:1 layers may differ in charge, with the total layer charge for a sample being an average of these different charges). Additional factors involved in the structural heterogeneity of smectites include cation ordering in the octahedral sheet, and *cis-trans* occupancy (Drits *et al.*, 1998; Cuadros *et al.*, 1999). The present paper describes a new XRD method that can be used to determine approximate total layer charge and layer-charge heterogeneity among smectite 2:1 layers. The technique does not address the problem of charge location (i.e. octahedral vs. tetrahedral charge).

Smectite total layer charge and the heterogeneity of this charge from layer to layer has been measured previously by a variety of methods, including: (1) microcalorimetry (Talibudeen and Goulding, 1983), in which the heat released during determination of an exchange isotherm is related to different types of exchange sites and hence to charge heterogeneity; (2) measurement of the structural formula using chemical or microbeam methods (Weaver and Pollard, 1973; Newman and Brown, 1987; Christidis and Dunham, 1993, 1997) in which the oxide content of a purified smectite sample is measured and then converted into a structural formula; and (3) by XRD analysis after saturation with inorganic or organic cations (Tettenhorst and Johns, 1966; Čičel and Machajdik, 1981; Stul and Mortier, 1974; Lagaly, 1981; 1994; Olis *et al.*, 1990).

All of these methods have shortcomings. The microcalorimetric method is difficult to apply without specialized equipment, and does not give total layer charge. The chemical methods, while potentially the most accurate for determining total layer charge, cannot determine layer-charge heterogeneity, and can be affected by the presence of impurities such as silica phases (quartz, opal-CT), other clay minerals, Fe oxides, or amorphous materials (Si, Al gels) in the clay fraction. These impurities can often be detected and quantified by XRD, or removed by chemical treatments (Jackson, 1985). The microbeam techniques for determining structural formulae (electron microprobe analysis, EMPA; analytical-transmission electron microscopy, AEM-TEM) are not considered to be accurate methods for charge characterization, either because of the existence of fine-grained impurities such as Fe, Mn, Ti

\* E-mail address of corresponding author:  
christid@mred.tuc.gr  
DOI: 10.1346/CCMN.2003.0510607

or amorphous oxides in close association with clays, because of analytical problems such as the volatilization of light elements, or because of experimental constraints and errors (*cf.* Velde, 1984; Warren and Ransom, 1992; Christidis and Dunham, 1993, 1997).

X-ray diffraction, which provides the most convenient set of methods, has been used extensively to determine total layer charge and the charge heterogeneity of smectites. In these methods, the clay fraction is either saturated with an inorganic cation of low hydration energy, preferably K, and subsequently treated with ethylene glycol (Tettenhorst and Johns, 1966; Čičel and Machajdik, 1981), or is saturated with alkylammonium ions (see Lagaly, 1994, for a review). Both methods assume that smectite is composed of a random interstratification of smectite 2:1 layers having different charges. The alkylammonium method does not recognize end-member smectite layers having distinct layer charges, but instead yields a continuous distribution of layer charges. By contrast, saturation with K yields three end-member layers with spacings of ~17, 14 and 10 Å, having layer charges of -0.28, -0.6 and -1.0 equivalents, respectively, per half unit-cell according to Tettenhorst and Johns (1966) and Machajdik and Čičel (1981). The approach of Tettenhorst and Johns calculates only relative proportions of different layers, and

not total charge. The alkylammonium method is by far the most widely used technique despite significant shortcomings which include difficulty in sample preparation and under- or overestimation of permanent layer charge of high- and low-charge smectites (Maes *et al.*, 1979; Laird *et al.*, 1989; see also Laird, 1994, for a review). The present contribution presents an alternative method for determination of smectite layer charge and charge distribution based on a comparison between XRD traces of K-saturated, ethylene glycol-solvated smectites and computer-simulated XRD traces calculated for three-component interstratification.

## MATERIALS AND METHODS

### Experimental methods

Twenty-eight smectites with known structural formulae were used in the present study (Table 1). A beidellite from Glen Silver Pit Idaho, with unknown structural formula was also examined. These smectites, which cover the entire range of smectite compositions (*cf.* Schultz, 1969; Newman and Brown, 1987), have variable layer charges, both with respect to location and magnitude. They were taken from the Leonard G. Schultz (LGS) collection, from the CMS clay repository, and from the collection of D.D. Eberl, and their total

Table 1. Origin and layer charge per half formula unit of the smectite used.

Smectite	Origin	Layer charge	Characterization
SWy-1	CMS repository	0.36 <sup>1</sup>	Wyoming-type motmorillonite
Hectorite	CMS repository	0.41 <sup>1</sup>	Hectorite
LGS#18	L.G. Schultz collection	0.38 <sup>2</sup>	Wyoming-type motmorillonite
Belle Fourche	D.D. Eberl collection	0.39 <sup>3</sup>	Wyoming-type motmorillonite
LGS#45	L.G. Schultz collection	0.40 <sup>2</sup>	Otay-type montmorillonite
LGS#5	L.G. Schultz collection	0.375 <sup>1</sup>	Wyoming-type motmorillonite
LGS#8	L.G. Schultz collection	0.40 <sup>2</sup>	Wyoming-type motmorillonite
LGS#61	L.G. Schultz collection	0.415 <sup>2</sup>	Chambers-type montmorillonite
Woburn	L.G. Schultz collection	0.42 <sup>2</sup>	Ferruginous montmorillonite
LGS#19	L.G. Schultz collection	0.42 <sup>2</sup>	Wyoming-type motmorillonite
Camp Berteau	D.D. Eberl collection	0.43 <sup>3</sup>	Chambers-type montmorillonite
LGS#54	L.G. Schultz collection	0.425 <sup>2</sup>	Chambers-type montmorillonite
Texas	CMS repository	0.44 <sup>2</sup>	Chambers-type montmorillonite
Montmorillon	D.D. Eberl collection	0.44 <sup>1</sup>	Tatavilla-type montmorillonite
LGS#50	L.G. Schultz collection	0.44 <sup>2</sup>	Chambers-type montmorillonite
Red Hill	L.G. Schultz collection	0.44 <sup>2</sup>	Ferruginous montmorillonite
LGS#59	L.G. Schultz collection	0.445 <sup>2</sup>	Chambers-type montmorillonite
LGS#57	L.G. Schultz collection	0.40 <sup>2</sup>	Chambers-type montmorillonite
Glen Silver Pit	D.D. Eberl collection	unknown	Beidellite
Black Jack	CMS repository	0.47 <sup>1</sup>	Beidellite
LGS#47	L.G. Schultz collection	0.485 <sup>2</sup>	Chambers-type montmorillonite
Kinney	D.D. Eberl collection	0.49 <sup>1</sup>	Otay-type montmorillonite
LGS#40	L.G. Schultz collection	0.52 <sup>2</sup>	Otay-type montmorillonite
LGS#39	L.G. Schultz collection	0.555 <sup>2</sup>	Otay-type montmorillonite
SAZ-1	CMS repository	0.555 <sup>1</sup>	Otay-type montmorillonite
LGS#35	L.G. Schultz collection	0.59 <sup>2</sup>	Chambers-type montmorillonite
Otay	CMS repository	0.60 <sup>1</sup>	Otay-type montmorillonite
LGS#42	L.G. Schultz collection	0.49 <sup>2</sup>	Otay-type montmorillonite
LGS#74	L.G. Schultz collection	0.675 <sup>2</sup>	Beidellite

Sources for layer-charge values: <sup>1</sup> Eberl *et al.* (1986), <sup>2</sup> Schultz (1969), <sup>3</sup> Newman (1987)

layer charges were determined from structural formulae calculated from chemical analyses (Schultz, 1969; Eberl *et al.*, 1986; Newman and Brown, 1987).

The smectites were dispersed in distilled water using an ultrasonic probe (for 20 s). The  $<2 \mu\text{m}$  fraction was separated by settling, and then saturated twice with K using 1 N KCl. The K-smectites were centrifuged, dialyzed until chloride free (silver nitrate test), dried on Si wafers at room temperature, and then were solvated with ethylene glycol vapor at 60°C overnight. Inasmuch as relative humidity may affect  $d$  spacings of mixed-layer phases containing an expandable component (Eberl *et al.*, 1987), all quantitative XRD methods, which use peak migration, are sensitive to error. Therefore maximum ethylene glycol saturation must be ensured. Also, since sample preparation affects hysteresis in the swelling of K-smectite, consistent preparation after K saturation is necessary. In this work we used air-dried samples without further treatment prior to ethylene glycol solvation. The XRD analysis was performed from 2 to  $35^\circ 2\theta$ , with a Siemens D500 XRD, using  $\text{CuK}\alpha$  radiation (40 kV, 30 mA), a graphite monochromator, a step size of  $0.02^\circ 2\theta$ , with 4 s count time per step. The scans were transferred to a computer using a Siemens Daco-MP interface, converted to MS Excel format, and loaded into the LayerCharge program (Eberl and Christidis, 2002), to be described below.

#### The LayerCharge program

The LayerCharge program was written using Visual Basic, the code employed by the macro function of Microsoft Excel<sup>®</sup>, to determine total layer charges and layer-charge distributions for 100% expandable smectites from XRD patterns of K-saturated, ethylene glycol-solvated samples. Upon K saturation and glycol treatment, three types of layers may form in such smectites. Based on computer modeling, these randomly interstratified layers have spacings of approximately 17.1 Å, 13.5 Å and 9.98 Å. These spacings are approximations, because, for example, the 17.1 Å spacing can vary from 17.3 to 16.6 Å (Środoń, 1980). The spacings used for the end-members were selected because they best modeled the peak positions found in the experimental patterns, especially with respect to the 005 reflections. The  $d$  spacing values of the three types of layers are assumed to be related to at least three different values for layer charge, with the lowest charge, 17.1 Å layers absorbing two glycol layers, the intermediately charged 13.5 Å layers absorbing one glycol layer, and the highest charged 9.98 Å layers being completely collapsed. The difference in extent of swelling for these three types of layers probably results from an interplay between layer charge and K ion hydration energy (Eberl, 1980).

Using Reynolds' 3-COMP program (Reynolds, 1985), 174 XRD patterns for randomly interstratified clay having various proportions of 17.1/13.5/9.98 Å layers were calculated from 2 to  $35^\circ 2\theta$ , with step sizes of

$0.1^\circ 2\theta$ . An Fe content of 0.1 atoms per half unit-cell was adopted for the calculated patterns. The crystallite size distribution used for this calculation was lognormal, using lognormal parameters determined from MudMaster analysis (Eberl *et al.*, 1996) of several Ca-saturated, glycol-solvated smectites ( $\alpha = 1.95$ ;  $\beta^2 = 0.25$ ). The 3-COMP calculated patterns were stored in the program, and were matched to the experimental pattern after removal of the Lorentz-polarization (Lp) factor (Moore and Reynolds, 1997) from both types of patterns. Removal of the Lp factor yields a more accurate spacing for the 001 peak, a spacing that is minimally shifted by the breadth of the XRD peak. This removal is considered to be important because for two peaks having the same  $d$  spacing value, the broader peak will be shifted to lower  $2\theta$  angles by the Lp factor. Calculated and measured patterns were matched either by matching peak positions for 00 $l$  reflections, or by whole-pattern fitting. These matches were accomplished by finding the calculated pattern which minimizes the sum of the squared differences between either the experimental and calculated peak positions for the first six 00 $l$  reflections, or for the whole-pattern fit of experimental and calculated XRD intensities that were normalized to the intensity of the most intense peak. Peaks can be removed from the analysis if they are not well defined, or if there are interferences with other phases, and the whole-pattern analysis routine can be terminated at any  $2\theta$  value up to  $35^\circ$ . The program automatically selects the calculated pattern which best matches the experimental profile. Once the calculated pattern has been found, the patterns are compared visually to ensure that they are similar. If the match is good, the relative proportion of the three types of layers has been determined. Matches generally are not perfect, possibly due to small variations in spacings for the three types of layers. Experimental patterns could be matched more exactly by detailed modeling (*cf.* Sakharov *et al.*, 1999), but the present method avoids this sometimes lengthy process for the sake of speed and convenience, while accepting that the solutions are approximate.

The next problem is to assign a charge to each layer type, and then to calculate the total layer charge of the clay. The 28 samples of known total layer charge were analyzed using the Solver option in Excel<sup>®</sup> to determine mean charges for the three types of layers. A charge for each type of layer was multiplied by the proportion of that layer found for each sample, and then the total layer charge for each sample was calculated. The charge for each type of layer was varied by Solver until the squared differences between the measured and calculated mean layer charges for the 28 samples were minimized. As will be discussed below, this led to mean charges of  $-0.39$ , and  $-0.42$  per half unit-cell for the 17.1 Å and 13.5 Å layers, respectively, and to two values for the 9.98 Å layers,  $-0.53$  and  $-0.76$  equivalents for the low- (type 1) and high- (type 2) charge smectites, respectively.

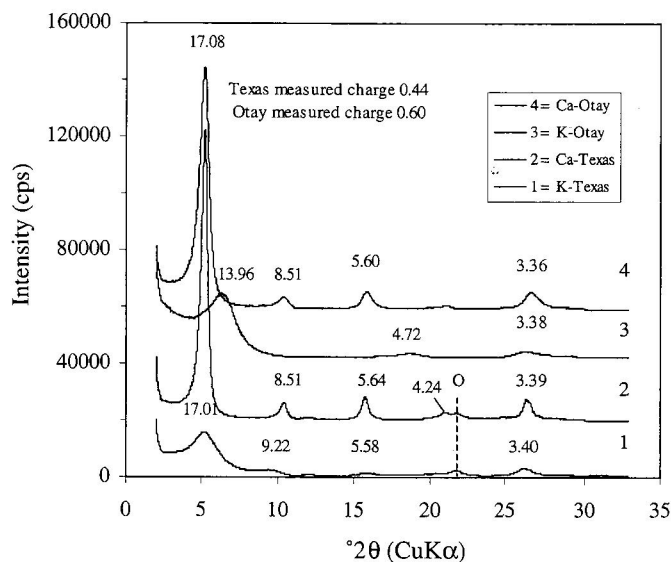


Figure 1. Representative XRD patterns of K- and Ca-saturated, ethylene glycol-solvated Texas and Otay smectites. O = opal CT.

## RESULTS

### XRD patterns of K-saturated smectites

Representative XRD patterns from oriented samples of two smectites having different total layer charges and saturated with  $\text{Ca}^{2+}$  and  $\text{K}^+$  ions are shown in Figure 1. Although all layers are fully expandable when saturated with  $\text{Ca}^{2+}$ , there are significant variations in layer spacings when the smectites were saturated with  $\text{K}^+$ . This behavior is well known from previous studies (e.g. Tettenhorst and Johns, 1966; Čičel and Machajdik, 1981; Sato *et al.*, 1992), and indicates that the use of the K-saturated form may reveal information about smectite layer-charge distributions.

Representative XRD patterns from oriented samples of K-saturated smectites are shown in Figure 2. Two different groups of smectites can be distinguished

according to their XRD patterns. In the first group, which essentially includes smectites having a small total layer charge, the first-order reflection ranges between 16 and 17.1 Å, and higher-order basal reflections usually are well defined (Figure 2a–d). These smectites can be classified further into two sub-types according to the shape and rationality of higher-order basal reflections. The first type (group 1a) includes those smectites with 001 *d* spacing values >16.6 Å, and which have, in general, a well defined and rational series of higher-order basal reflections (Figure 2a,b). Typical examples of group 1a are SWy-1, hectorite, Belle Fourche, Woburn and smectites from samples 8, 18, 19 and 45 from the LGS collection. Most of these smectites are classified as Wyoming-type smectites according to Schultz (1969). The second type (group 1b) includes

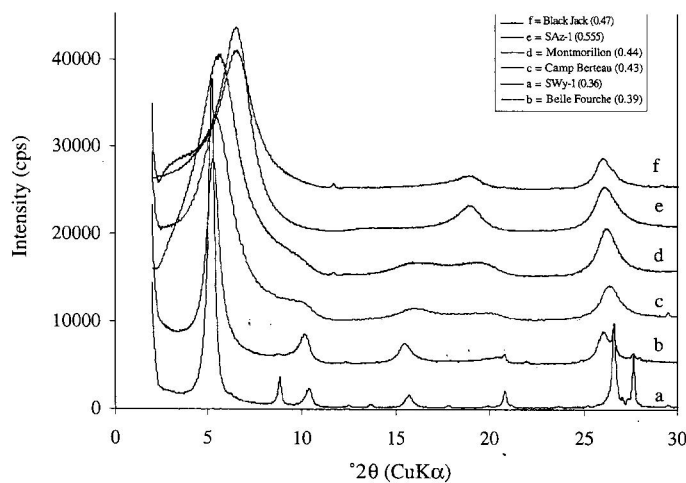


Figure 2. Representative XRD patterns of K-saturated, ethylene glycol-solvated smectites classified into group 1a (a,b), group 1b (c,d) and group 2 (e,f). See text for definition of groups 1a, 1b and 2. Values in brackets are measured layer charges.

smectites with 001  $d$  spacing values ranging between 16 and 16.6 Å that have irrational higher-order basal reflections. Also, the 002 reflection for this type of smectite is usually a shoulder. Typical examples of group 1b are the montmorillonites from Camp Berceau, Montmorillon and Red Hill, and a beidellite from Glen Silver Pit.

The second type of smectite (group 2) includes typically high-charge smectites, and is characterized by first-order reflections between 15.5 and 13.5 Å, and a 003 reflection at 4.65–4.70 Å which tails off with a shoulder at the low-angle side (Figure 2e,f). Examples of group 2 are SAz-1, Otay and Kinney montmorillonites in samples 35, 36, 40 and 47 from the LGS collection, and beidellites including the Black Jack and sample 74 from the LGS collection. Polkville is also included in this group although its 001 reflection occurs at 15.85 Å because of the shape and positions of its remaining basal reflections. Both type 1 and type 2 groups contain montmorillonite and beidellite. Smectites from both groups fully expanded to  $\sim 17$  Å when saturated with  $\text{Na}^+$  or bivalent cations ( $\text{Ca}^{2+}$ ,  $\text{Ba}^{2+}$ ) and glycol solvated.

The first- and second-order basal reflections of the calculated patterns are sensitive to the proportion of the 17.1 Å layers (Figure 3;  $R^2 = 0.85$  and 0.88, respectively, for a linear correlation). The first-order reflection migrates to smaller  $d$  spacing values with a decreasing proportion of 17.1 Å layers, whereas the second-order reflection follows an opposite trend. Both of these trends are observed in smectites containing at least 20% 17.1 Å layers. For smaller proportions of 17.1 Å layers the trends are not obvious. The limit at 20% 17.1 Å layers also marks the average proportion of 17.1 Å layers found in high-charge (group 2) smectites (see below). The migration of the first and second peaks is used in the LayerCharge program to provide an approximate and independent estimation of the proportion of 17.1 Å layers. By contrast, the  $d$  spacing values of the higher-order basal reflections do not bear systematic relationships with the proportion of 17.1 Å layers. Also, with the possible exception of the third-order reflection which displays limited sensitivity to the proportion of the 13.5 Å layers ( $R^2 = 0.75$ ), the positions of the other basal reflections are not sensitive to variations in the propor-

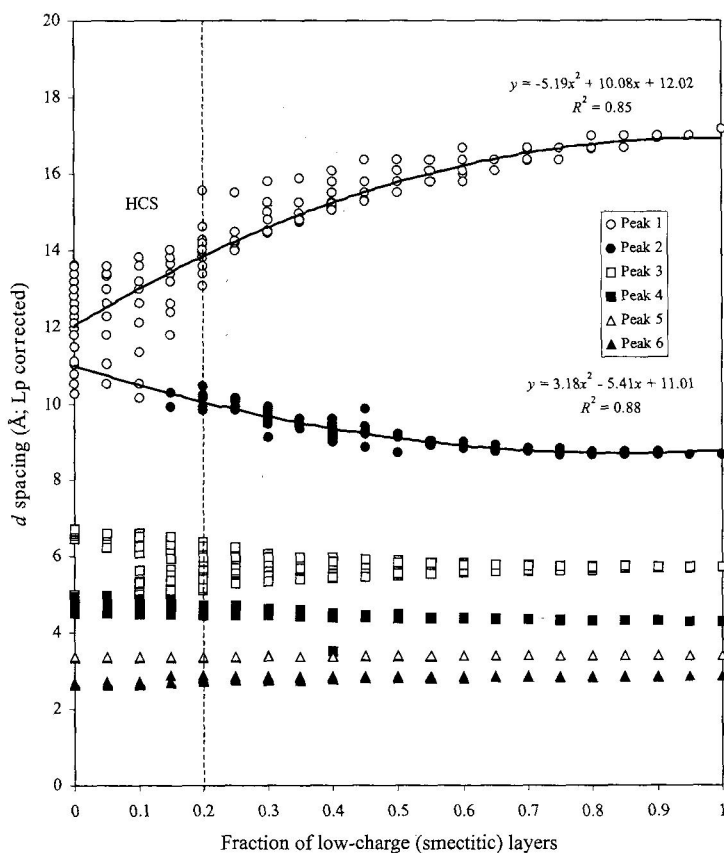


Figure 3. Migration of basal reflections of the calculated traces of K-saturated ethylene glycol-solvated smectites as a function of low-charge layers. The dashed line separates high-charge smectites (HCS). Peak 1 is the  $(001)_{17.1 \text{ \AA}} / (001)_{13.5 \text{ \AA}}$  reflection, Peak 2 is the  $(002)_{17.1 \text{ \AA}} / (001)_{13.5 \text{ \AA}} / (001)_{9.98 \text{ \AA}}$  reflection, Peak 3 is the  $(003)_{17.1 \text{ \AA}} / (002)_{13.5 \text{ \AA}} / (002)_{9.98 \text{ \AA}}$  reflection, Peak 4 is the  $(004)_{17.1 \text{ \AA}} / (003)_{13.5 \text{ \AA}} / (002)_{9.98 \text{ \AA}}$  reflection, Peak 5 is the  $(005)_{17.1 \text{ \AA}} / (004)_{13.5 \text{ \AA}} / (003)_{9.98 \text{ \AA}}$  reflection and Peak 6 is the  $(006)_{17.1 \text{ \AA}} / (005)_{13.5 \text{ \AA}} / (004)_{9.98 \text{ \AA}}$  reflection.

tion of the 13.5 and 9.98 Å layers. An attempt to use the position of the third reflection to estimate the proportion of 13.5 Å layers, and subsequently the proportion of 9.98 Å layers by difference, was not successful.

The K-smectites in samples 5 and 23 from the LGS collection display an additional reflection at 13.8–14 Å (Figure 4). Duplicate oriented mounts, prepared to avoid incomplete ethylene glycol saturation, confirmed the existence of this additional reflection. Since chlorite is not present, this reflection is attributed either to vermiculite or to a high-charge (group 2) smectite, either montmorillonite or beidellite. After Mg saturation and glycerol solvation, the reflection disappeared in sample 5 but not in sample 23 (Figure 4). Therefore in sample 5 the 14 Å reflection is attributed to high-charge smectite, which expands to 17.8 Å after Mg saturation and glycerol solvation. In sample 23 this reflection is attributed to vermiculite, because Mg-vermiculite does not expand after glycerol solvation (Walker, 1961). This operational definition separates high-charge smectites from vermiculites. Vermiculite in sample 23 is probably associated with degradation of biotite mica present in this sample (Schultz, 1969).

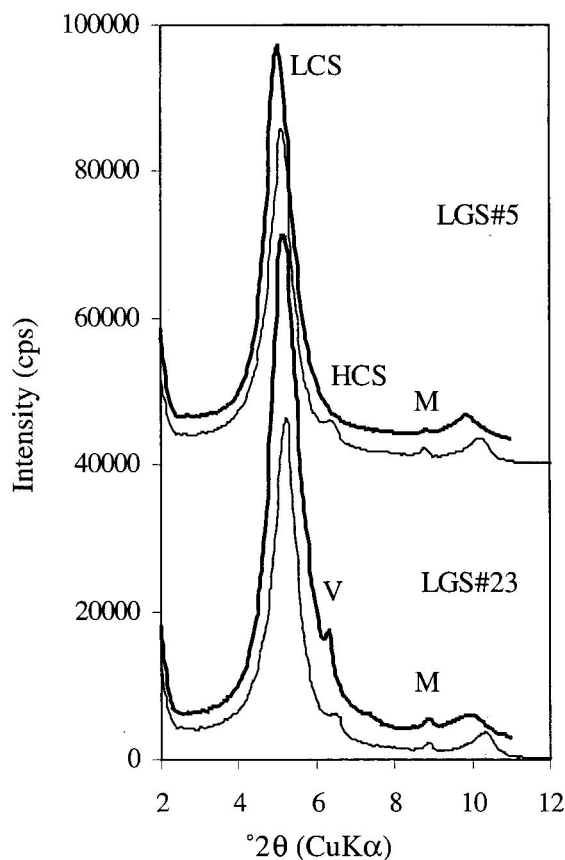


Figure 4. Ethylene glycol- (thin line) and glycerol-solvated (thicker line) K-smectites from samples 5 and 23 of the L.G. Schultz collection. LCS = low-charge smectite, HCS = high-charge smectite, V = vermiculite, M = mica.

#### Determination of layer charge of smectites

Previous work on determination of the layer charge of smectites after saturation with cations of low hydration energy (Tettenhorst and Johns, 1966; Čičel and Machajdik, 1981; Machajdik and Čičel, 1981) assumes that the three types of smectite layers have constant layer charges. The constant layer charge concept was initially followed in the present study. However, the use of the end-member charges adopted by Machajdik and Čičel (1981) for our samples yielded unreasonably large layer charges for the high-charge smectites and charges that were too small for the low-charge smectites. A first approximation for the values of constant end-member charges using the Solver program yielded a linear trend with a correlation coefficient  $R^2 = 0.76$ , and charges of  $-0.36$ ,  $-0.49$  and  $-0.66$  for the 17.1, 13.5 and 9.98 Å layers, respectively (Figure 5a). It is obvious that the relationship between the measured and the calculated layer charges has a breaking point, which separates low- from high-charge smectites, at a layer charge of  $-0.46$  per half unit-cell (Figure 5b). This value is comparable to  $-0.43$  usually accepted as a boundary between the low- and the high-charge smectites (e.g. Newman and Brown, 1987). It is also observed that plotting the charges in this manner yields two lines, not a single line, and that the lines do not pass through the origin with a slope close to 1, as would be expected if the approach were correct.

The next step in the Solver analysis was to allow the charge of the three types of layers to vary separately for the low- and high-charge smectites (Table 2). A well defined linear relationship ( $R^2 = 0.95$ ) was observed between the measured and the calculated layer charges throughout the entire layer charge range, and the regression line with a slope of 1 passes through the origin (Figure 5c). Most important, it was found that although the charges of the 17.1 and 13.5 Å layers were essentially equal for the low- and high-charge smectites ( $-0.38$  vs.  $0.39$ , and  $-0.46$  vs.  $-0.42$ ), the charge of the 9.98 Å layers was significantly larger in the high-charge smectites ( $-0.76$  compared to  $-0.53$  for the low-charge smectites). This important outcome contrasts with the findings of Talibudeen and Goulding (1983) who observed heterogeneity in low-charge layers, but relative homogeneity in high-charge layers using microcalorimetry. The final layer charges obtained for the three types of layers, listed in Table 2, were found by assigning single charges to 17.1 and 13.5 Å layers (which, after the Solver solution, were found to be  $-0.39$  and  $-0.42$ , respectively), but two separate charges for low- and high-charge smectites for the 9.98 Å layers (which were found to be  $-0.53$  and  $-0.76$ , respectively). In addition, two samples (LGS#74 and Black Jack beidellite), did not fit this model (Figure 5b). When we allowed their charges to vary separately during the Solver solution, they yielded charges of  $-1.0$  and  $-0.54$ , respectively, for the 9.98 Å layers. Note that the value of

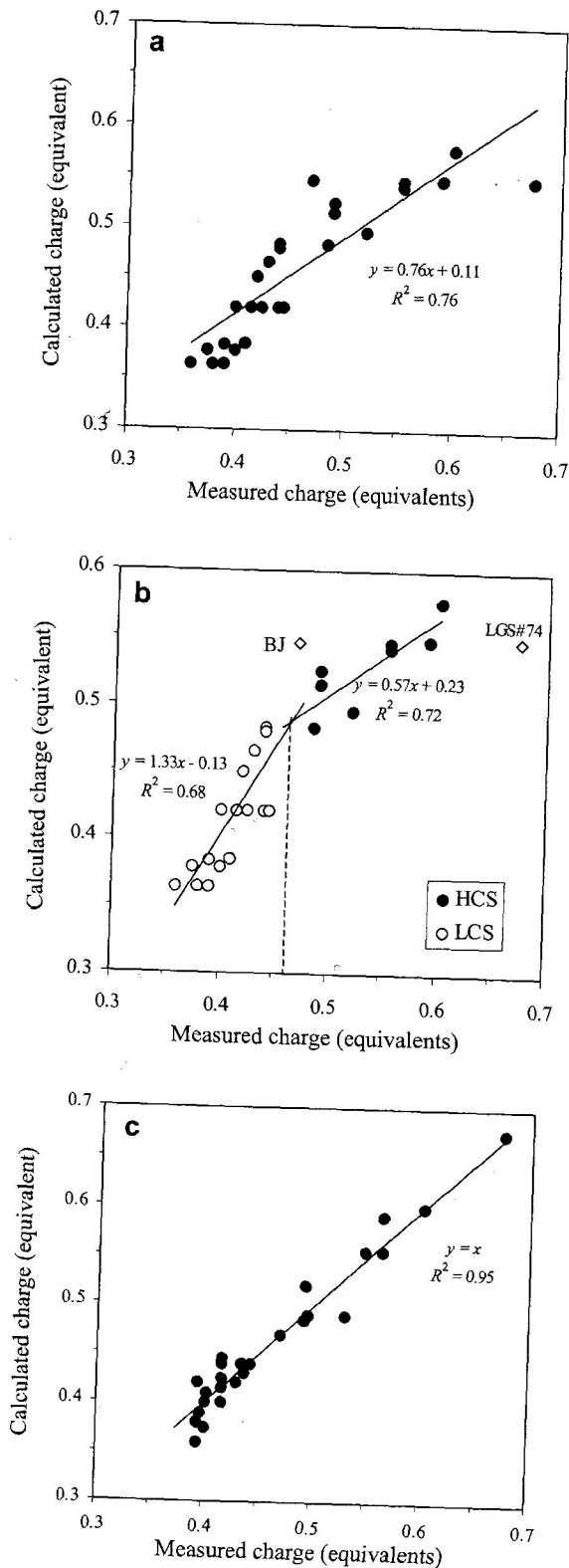


Figure 5. Measured vs. calculated layer charge of smectites using the LayerCharge program (Eberl and Christidis, 2002). (a) Overall relationship assuming constant charge for the 17.1 Å, 13.5 Å and 9.98 Å peaks (-0.36, -0.49 and -0.66,

-0.54 obtained for the 9.98 Å layers of Black Jack is almost identical to the charge of 9.98 Å layers for low-charge smectites (Table 2).

The calculated total layer charges for the examined smectites are listed in Table 3. The proportion of 17.1 Å layers for the low- and high-charge smectites are clearly different. Smectites from the low-charge group 1 consist of 77% 17.1 Å layers on average, whereas those from the high-charge group 2 smectites contain only an average of 20% 17.1 Å layers (Table 3). Unlike previous studies (Machajdik and Čičel, 1981), there is a close agreement between calculated and measured charges. Also, the proportion of the different types of layers determined for sample LGS#50 is comparable to the value given by Tettenhorst and Johns (1966) using the Fourier transform method (Table 3). Typical examples of XRD profile fitting using the LayerCharge program (Eberl and Christidis, 2002) are shown for Texas, Montmorillon and Otay smectites (Figure 6). Texas is a group 1a smectite, Montmorillon a group 1b smectite and Otay is a group 2 smectite.

There is a relation between the total charges calculated using the LayerCharge program and *d* spacing values of the 001 reflections (Figure 7). Once again, low- and high-charge smectites are separated. The low-charge smectites display considerably less scatter in Figure 7 compared to their high-charge counterparts, probably due to variation in the charge of the 9.98 Å layers. Black Jack beidellite and sample LGS#74 do not follow this trend. Black Jack beidellite is a unique sample, modeled by assuming 50% 13.5 Å layers and 40% 9.98 Å layers having a charge of -0.54, whereas sample LGS#74 was modeled by assuming a charge close to -1.0 for the high-charge layers, comparable to that of true mica (Table 3). Also, smectite from Montmorillon, France, plots outside the field of low-charge smectites, because its 001 spacing is 15.15 Å. The boundary between the two types of smectite seems to be at a layer charge of -0.46, almost identical to the breaking point of the linear trends in Figure 5b. Therefore, according to the results of this study, the layer-charge boundary between low- and high-charge smectites is -0.46 per half unit-cell, with the 001 reflection boundary at 15.5 Å.

## DISCUSSION

The LayerCharge program can be applied successfully for calculation of the total layer charge and the

respectively); (b) separation of the low-charge smectites from the high-charge smectites at layer charge of -0.46; (c) relationship assuming constant charge for the 17.1 Å and 13.5 Å layers in all smectites (-0.39 and -0.42, respectively) and different charge for the 9.98 Å layers in the low-charge smectites and high-charge smectites (-0.53 and -0.76, respectively). Black Jack (BJ) and LGS#74 (both beidellites) do not follow the observed trends.

Table 2. Layer charge of the different types of layers of smectites determined with the program LayerCharge (Eberl and Christidis, 2002) using Solver. Values in brackets indicate average charges of the different layers for the high-charge smectites.

Approach used for calculation of layer charge	Low-charge layers (17.1 Å)	Medium-charge layers (13.5 Å)	High-charge layers (10 Å)
Constant charge for the end-members	0.36	0.49	0.66
Different charge of end-members for low- and high-charge smectites	0.38 (0.39)	0.46 (0.42)	0.53 (0.76)

layer-charge distribution of smectites. The proposed method uses either a peak position method or a whole-profile fitting method to find the calculated pattern that best matches the measured pattern. The peak position method may be less accurate for the high-charge smectites, because the position calculated for the 005 reflection, and sometimes that calculated for the 001 reflection, are not always accurate for these clays. In these instances, the whole-profile fitting method is used. By contrast, the presence of other clay minerals or non-clay minerals with diffraction maxima in the proximity of K-smectite maxima (e.g. illite, quartz) may lead to the selection of an incorrect calculated pattern if the whole-profile fitting option is selected, resulting in a poor fit. In this case, the peak-fitting option is preferred. For the majority of smectites that we have examined, both approaches yield a similar result, which differs by <5% in the distribution of the different types of layers. The influence of this difference in determination of layer charge is negligible, and does not exceed 2%. Therefore, either of the two methods can be used for layer-charge determination. Currently the technique is used exclusively for smectites, and its applicability for samples

containing randomly interstratified mixed-layer illite-smectite (I-S) is under investigation.

The overall error for determination of the total average layer charge does not exceed 3.5% at a layer charge of 0.50 per half unit-cell. Therefore, this rapid method yields a good approximation for the layer charge of smectites. It can provide a large amount of good quality data easily, and should be useful both for basic research and for industrial purposes. As was mentioned previously, the method does not address the influence of charge site (tetrahedral vs. octahedral charge) in layer-charge determination (e.g. Sato *et al.*, 1992). This deficiency could be a source of error, because tetrahedral charge affects the swelling of layers, and may partially contribute to the observed discrepancy between the measured and the calculated layer charge values even for low-charge smectites (Figure 5c). The main limitation of the method involves difficulty in simulation of unusual samples such as Black Jack and LGS#74, both beidellites, with extreme charges for the 9.98 Å layers (−0.54 and −1.0 respectively). Thus, the presence of a large proportion of 9.98 Å layers with extremely high or low charge in some high-charge smectites or the

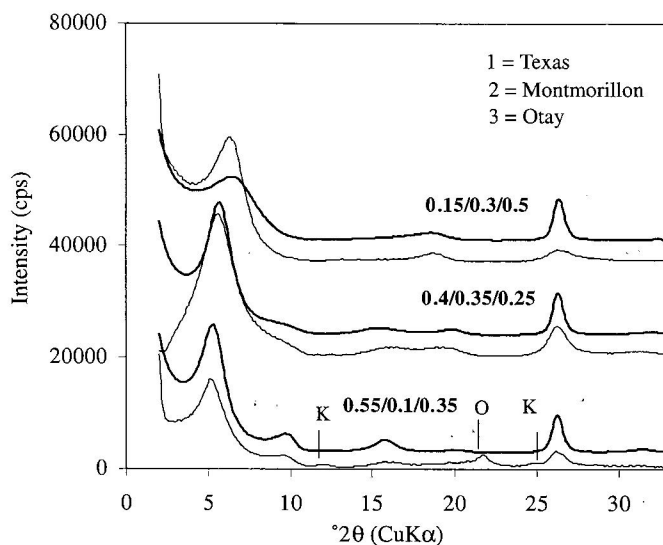


Figure 6. Profile fitting of the K-saturated Texas, Montmorillon and Otay smectites. K = kaolinite, O = Opal CT. Regular lines correspond to experimental and bold lines to calculated patterns. The fitting of the 001 reflection of the K-Otay smectite is not good, but the rest of the profile fits well.



Table 3. Fraction of the low-, intermediate- and high-charge layers (17, 13.5 and 10 Å, respectively), calculated and measured layer charge and  $d_{001}$  spacing of the smectites studied. No. of illite layers after 100 wetting and drying (WD) cycles are from Eberl *et al.*, (1986). LGS# denotes samples from the L.G. Schultz collection. Values in brackets (LGS#50) are percentages of layers determined by Tettenhorst and Johns (1966).

Smectite	Fraction of 17.1 Å layers	Fraction of 1.5 Å layers	Fraction of 9.98 Å layers	Charge of 9.98 Å layers	Calculated layer charge (LayerCharge)	Measured layer charge (structural formula method)	Difference between the two methods	$d$ spacings of the 001 reflection	% of illite layers after 100 WD cycles
Low-charge smectites									
SWy-1	1	0	0	0	0.394	0.360	0.034	17.04	8
Hectorite	0.9	0.05	0.05	1.000	0.402	0.410	0.008	16.92	12
LGS#18	1	0	0	0	0.394	0.380	0.014	17.20	
LGS#5	0.95	0	0.05	0.478	0.401	0.375	0.026	17.15	
Belle Fourche	0.85	0.15	0	0	0.397	0.390	0.007	16.66	
LGS#45	0.75	0.1	0.15	0.495	0.416	0.400	0.016	16.48	
LGS#8	0.95	0	0.05	0.907	0.401	0.400	0.001	17.08	
LGS#61	0.75	0.1	0.15	0.591	0.416	0.415	0.001	16.11	
Woburn	0.65	0.1	0.25	0.567	0.430	0.420	0.010	16.17	
LGS#19	1	0	0	0	0.394	0.420	0.026	17.11	
Camp Berteau	0.6	0.1	0.3	0.603	0.436	0.430	0.006	16.11	
LGS#54	0.75	0.1	0.15	0.654	0.416	0.425	0.009	16.15	
Texas	0.55	0.1	0.35	0.642	0.443	0.440	0.003	16.21	22
Montmorillon	0.4	0.35	0.25	0.62	0.434	0.440	0.006	15.15	27
LGS#50	0.75(0.73)	0.15(0.19)	0.10(0.08)	0.75	0.416	0.440	0.024	16.68	
Red Hill	0.55	0.1	0.35	0.642	0.443	0.440	0.003	15.66	
LGS#59	0.75	0.1	0.15	0.782	0.416	0.445	0.029	16.60	
LGS#57	0.75	0.1	0.15	0.623	0.416	0.450	0.034	16.58	
Glen Silver Pit	0.4	0.25	0.35	—	0.445	—	—	15.52	
High-charge smectites									
Black Jack	0.1	0.5	0.4	0.57	0.470	0.470	0.003	13.18	43
LGS#47	0.4	0.35	0.25	0.695	0.491	0.485	0.006	15.44	
Kinney	0.2	0.45	0.35	0.735	0.529	0.49	0.039	13.63	33
LGS#40	0.3	0.45	0.25	0.751	0.493	0.520	0.027	15.23	
LGS#39	0.2	0.35	0.45	0.740	0.564	0.555	0.009	15.12	
SAz-1	0.1	0.5	0.4	0.715	0.548	0.555	0.007	13.20	41
LGS#35	0.15	0.4	0.45	0.656	0.565	0.590	0.025	13.71	
Otay	0.05	0.4	0.55	0.691	0.601	0.600	0.001	13.53	51
LGS#42	0.15	0.6	0.25	0.657	0.495	0.600	0.005	13.58	
LGS#74	0.15	0.4	0.45	1.00	0.674	0.675	0.001	13.97	
High-charge smectites (ave)	0.189	0.433	0.378						
Low-charge smectites (ave)	0.772	0.086	0.142						

Ave = average values

predominance of tetrahedrally charged sheets may decrease the accuracy of layer-charge determination, leading to an over- or underestimation by as much as 13%. However, such samples are rather exceptional, and, most importantly, accuracy in measuring the distribution of the different types of layers is not affected. The influence of tetrahedral charge on the precision of the method is currently under investigation.

According to their XRD patterns, the K-saturated smectites can be separated into two main groups, low- and high-charge smectites. A preliminary estimation of the layer charge of a smectite can be obtained merely by classification into group 1a and 1b (low charge) or group 2 (high charge). Hence group 1a smectites have layer charge  $<0.41$  per half unit-cell, group 1b smectites have layer charge between 0.42 and 0.46 per half unit-cell, and group 2 smectites have layer charge  $>0.46$  per half unit-cell. The layer charge boundary between group 1a and group 1b smectites is comparable to the boundary between high and low-charge smectites proposed by Newman and Brown (1987), *i.e.*  $-0.43$ . Thus according to the Newman and Brown scheme, group 1b smectites are high-charge smectites, which is not the case in the present work.

The main difference between low- and high-charge smectites is the proportion of 17.1 Å layers and 9.98 Å layers. Most Wyoming smectites and hectorite consist almost entirely of 17.1 Å layers (Table 3), and their unique swelling properties are attributed to the presence of these low-charge layers. Therefore it is suggested that the proportion of 17.1 Å layers dictates the quality of a bentonite deposit, *i.e.* its expected performance in industrial applications (*cf.* Inglethorpe *et al.*, 1993; Christidis and Scott, 1996). Thus the physical properties of two smectites that have a similar crystal chemistry (*e.g.* Wyoming *vs.* Chambers-type montmorillonites;

Güven, 1988) may be very different if they have different proportions of low- and high-charge layers.

The relative proportion of the different types of layers may affect the behavior of smectites during weathering. The amount of illite-like layers formed after 100 wetting and drying cycles and subsequent Sr saturation (Eberl *et al.*, 1986) is proportional to the amount of 9.98 Å layers and inversely proportional to the amount of 17.1 Å layers (Figure 8) as determined by the present technique. Hence the presence of high-charge layers accelerates the formation of illite-like layers during subsequent wetting and drying cycles in the presence of a K source. It is not known if this relation between the amount of 9.98 Å layers and degree of illitization can be extended to diagenetic or hydrothermal environments.

The 13.5 Å and 9.98 Å layers formed in K-saturated smectite should not be confused with vermiculite and/or mica-type minerals, as has been observed previously (*e.g.* Table 1 of Machajdik and Čičel, 1981). High-charge smectites expand to 17.8 Å after Mg saturation and glycerol solvation, whereas Mg-vermiculite continues to yield a  $d_{001}$  spacing of 14 Å (Figure 3). Also, Black Jack, an ideal beidellite (*i.e.* location of the tetrahedral charge is similar to vermiculite and mica), is a high-charge smectite (Figure 2), and its XRD trace was modeled with 10% 17.1 Å layers, 50% 13.5 Å layers, and 40% 9.98 Å layers (Table 3). Yet its measured layer charge is significantly  $<-0.6$ , which is the lower limit for vermiculite (Newman and Brown, 1987). Thus the 13.5 Å and 9.98 Å layers in the Black Jack clay are clearly distinct from vermiculitic and mica layers. Also, in high-charge smectites, the average charge of 9.98 Å layers was  $-0.76$  (Table 2) rather than  $-1.0$  for mica,

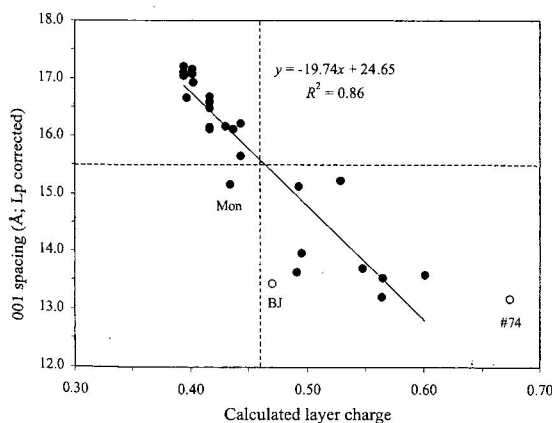


Figure 7. Relationship between calculated layer charge and 001 spacing of K-saturated smectites. LCS = low-charge smectites, HCS = high-charge smectites, BJ = Black Jack beidellite, #74 Sample 74 from the L.G. Schultz collection, Mon = Montmorillonite. The dashed lines separate low- from high-charge smectites according to their layer charge and  $d_{001}$  spacing.

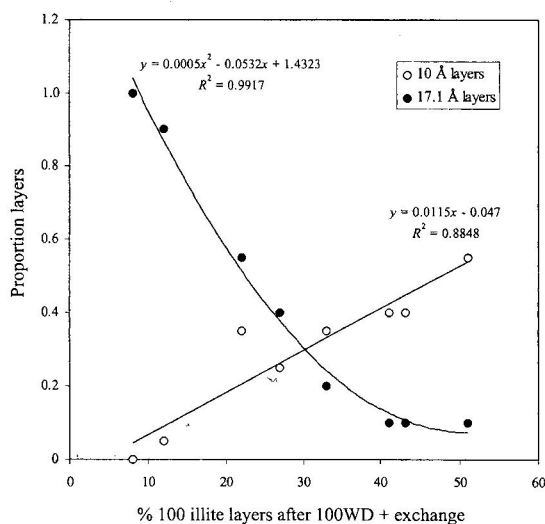


Figure 8. Dependence of formation of illite layers on the proportion of 17.1 Å and 9.98 Å layers of K-smectites after 100 wetting and drying (WD) cycles and subsequent exchange with Sr (data from Eberl *et al.*, 1986).

although in some samples the charge of 9.98 Å layers may be comparable to mica (e.g. LGS#74). Expansion of such fully charged layers to 17.1 Å after Ca saturation and ethylene glycol solvation may indicate either non-symmetric localization of the charge in the tetrahedral sheet (Tettenhorst and Johns, 1966) or a predominance of octahedral charge.

## CONCLUSIONS

Layer charge and charge distribution of smectites can be determined in K-saturated, ethylene glycol-solvated, oriented samples by analysis of XRD patterns using the LayerCharge program. The method utilizes the different degree of swelling of smectite layers depending on layer charge and charge distribution. The method is faster than previous techniques; it yields layer-charge values comparable to the structural formula method; and it is not affected by impurities. It can provide valuable information about the evolution of the layer charge of smectites during important geological processes such as illitization during wetting and drying and during diagenesis. Also, it can be used to assess the influence of layer charge and charge distribution on the physical properties of smectites, such as swelling and viscosity and thus on industrial applications. The method can be refined further by evaluation of the influence of charge localization on determination of layer charge.

## ACKNOWLEDGMENTS

This work was supported by a Fulbright Award to GEC to visit Boulder. J. Srodoń and A. Blum reviewed an earlier version of this script. The research could not have been completed without the bentonite collection of L.G. Schultz, given upon his retirement from the USGS, to DDE. The constructive comments of D.M. Moore, B. Velde, D.A. Laird, an anonymous referee and the editor improved the text. The use of trade names is for identification purposes only and does not constitute endorsement by the US Geological Survey.

## REFERENCES

- Christidis, G. and Dunham, A.C. (1993) Compositional variations in smectites derived from intermediate volcanic rocks. A case study from Milos Island, Greece. *Clay Minerals*, **28**, 255–273.
- Christidis, G. and Dunham, A.C. (1997) Compositional variations in smectites. Part II: Alteration of acidic precursors. A case study from Milos Island, Greece. *Clay Minerals*, **32**, 255–273.
- Christidis, G. and Scott, P.W. (1996) Physical and chemical properties of the bentonite deposits of Milos Island, Greece. *Transactions of the Institute of Mining and Metallurgy B*, **105**, B165–B174.
- Čičel, V. and Machajdik, D. (1981) Potassium- and ammonium-treated montmorillonites. I. Interstratified structures with ethylene glycol and water. *Clays and Clay Minerals* **29**, 40–46.
- Cuadros, J., Sainz-Diaz, C.I., Ramirez, R. and Hernandez-Laguna, A. (1999) Analysis of Fe segregation in the octahedral sheet of bentonitic illite-smectite by means of FTIR, <sup>27</sup>Al MAS NMR and reverse Monte Carlo simulations. *American Journal of Science*, **299**, 289–308.
- Decarreau, A., Colin, F., Herbillon, A., Manceau, A., Nahon D., Paquet, H., Trauth-Badeaud, D. and Trescases, J.J. (1987) Domain segregation in Ni-Fe-Mg-smectites. *Clays and Clay Minerals*, **35**, 1–10.
- Drits, V.A., Lindgreen, H., Salyn, A.L., Ylagan, R. and McCarty, D.K. (1998) Semi quantitative determination of trans-vacant and cis-vacant 2:1 layers in illites and illite-smectites by thermal analysis and X-ray diffraction. *American Mineralogist*, **83**, 1188–1198.
- Eberl, D.D. (1980) Alkali cation selectivity and fixation by clay minerals. *Clays and Clay Minerals*, **28**, 161–172.
- Eberl, D.D. and Christidis, G. (2002) *LayerCharge: A computer program for calculation of layer charge and charge distribution of smectites*. USGS, Boulder, Colorado.
- Eberl, D.D., Srodoń, J. and Northrop, R. (1986) Potassium fixation in smectite by wetting and drying. Pp. 296–326 in: *Geochemical Processes at Mineral Surfaces* (J.A. Davis and K.F. Hayes, editors). ACS Symposium Series **323**, American Chemical Society, Washington, D.C.
- Eberl, D.D., Srodoń, J., Mingchou L., Nadeau P.H. and Northrop, R.H. (1987) Sericite from the Silverton caldera, Colorado: Correlation among structure, composition, origin and particle thickness. *American Mineralogist*, **72**, 914–934.
- Goodman, B.A., Nadeau, P.H. and Chadwick, J. (1988) Evidence for the multiphase nature of bentonites from Mössbauer and EPR spectroscopy. *Clay Minerals*, **23**, 147–159.
- Güven, N. (1988) Smectite. Pp. 497–559 in: *Hydrous Phyllosilicates* (S.W. Bailey, editor). Reviews in Mineralogy, **19**. Mineralogical Society of America, Washington, D.C.
- Inglethorpe, S.D.J., Morgan, D.J., Highley, D.E. and Bloodworth, A.D. (1993) *Industrial Minerals laboratory manual: bentonite*. British Geological Survey Technical Report **WG/93/20**.
- Iwasaki, T. and Watanabe, T. (1988) Distribution of Ca and Na ions in dioctahedral smectites and interstratified dioctahedral mica/smectites. *Clays and Clay Minerals*, **36**, 73–82.
- Jackson, M.L. (1985) *Soil Chemical Analysis – Advanced Course*, 2<sup>nd</sup> edition. Published by the author, Madison, Wisconsin, 895 pp.
- Lagaly, G. (1981) Characterization of clays by organic compounds. *Clay Minerals*, **16**, 1–21.
- Lagaly, G. (1994) Layer charge determination by alkylammonium ions. Pp. 2–46 in: *Layer Charge Characteristics of 2:1 Silicate Clay Minerals* (A.R. Mermut, editor). CMS Workshop lectures, **6**. The Clay Minerals Society, Boulder Colorado.
- Lagaly, G. and Weiss, A. (1975) The layer charge of smectitic layer silicates. *Proceedings of the International Clay Conference Mexico*, 157–172.
- Laird, D.A. (1994) Evaluation of the structural formula and alkylammonium methods of determining layer charge. Pp. 80–103 in: *Layer Charge Characteristics of 2:1 Silicate Clay Minerals* (A.R. Mermut, editor). CMS Workshop lectures, **6**. The Clay Minerals Society, Boulder Colorado.
- Laird, D.A., Scott, A.D. and Fenton, T.E. (1989) Evaluation of the alkylammonium method of determining layer charge. *Clays and Clay Minerals*, **37**, 41–46.
- Lim, C.H. and Jackson, M.L. (1986) Expandable phyllosilicate reactions with lithium on heating. *Clays and Clay Minerals*, **34**, 346–352.
- MacEwan, D.A.C. and Wilson, M.J. (1984) Interlayer and intercalation complexes of clay minerals. Pp. 197–248 in: *Crystal Structures of Clay Minerals and their X-ray Identification* (G.W. Brindley and G. Brown, editors). Monograph **5**. Mineralogical Society, London.

- Machajdik, D. and Čičel, V. (1981) Potassium- and ammonium-treated montmorillonites. II. Calculation of characteristic layer charges. *Clays and Clay Minerals*, **29**, 47–52.
- Maes, A. and Cremers, A. (1977) Charge density effects in ion exchange. Part 1. Heterovalent exchange equilibria. *Faraday Transactions of the Royal Society of Chemistry*, **73**, 1807–1814.
- Maes, A., Stul, M.S. and Cremers, A. (1979) Layer charge-exchange capacity relationships in montmorillonite. *Clays and Clay Minerals*, **27**, 387–392.
- Moore, D.M. and Reynolds, R.C., Jr. (1997) *X-ray Diffraction and the Identification and Analysis of Clay Minerals*, 2<sup>nd</sup> edition. Oxford University Press, New York.
- Nadeau, P.H., Farmer, V.C., McHardy, W.J. and Bain, D.C. (1985) Compositional variations of the Unterrupstoth beidellite. *American Mineralogist*, **70**, 1004–1010.
- Newman, A.C.D. and Brown, G. (1987) The chemical constitution of clays. Pp. 1–128 in: *Chemistry of Clays and Clay Minerals* (A.C.D Newman, editor). Mineralogical Society, London.
- Olis, A.C., Malla, P.B. and Douglas, L.A. (1990) The rapid estimation of the layer charges of 2:1 expanding clays from a single alkylammonium ion expansion. *Clay Minerals*, **25**, 39–50.
- Reynolds, R.C., Jr. (1985) NEWMOD<sup>®</sup>, a computer program for the calculation of one-dimensional diffraction patterns of mixed-layer clays. R.C. Reynolds, Jr., 8 Brook Dr., Hanover, NH 03755.
- Sakharov, B.A., Lindgreen, H., Salyn, A. and Drits, V.A. (1999) Determination of illite-smectite structures using multispecimen X-ray diffraction profile fitting. *Clays and Clay Minerals*, **47**, 555–566.
- Sato, T., Watanabe, T. and Otsuka, R. (1992) Effects of layer charge, charge location and energy change on expansion properties of dioctahedral smectites *Clays and Clay Minerals*, **40**, 103–113.
- Schultz, L.G. (1969) Lithium and potassium adsorption, dehydroxylation temperature and structural water content of aluminous smectites. *Clays and Clay Minerals*, **17**, 115–149.
- Šrodoň, J. (1980) Precise identification of illite/smectite interstratifications by X-ray powder diffraction: *Clays and Clay Minerals*, **28**, 401–411.
- Stul, M.S. and Mortier, W.J. (1974) The heterogeneity of the charge density in montmorillonites. *Clays and Clay Minerals*, **22**, 391–396.
- Talibudeen, O. and Goulding, K.W.T. (1983) Charge heterogeneity in smectites. *Clays and Clay Minerals*, **31**, 37–42.
- Tettenhorst, R. and Johns, W.D. (1966) Interstratification in montmorillonite. *Clays and Clay Minerals*, **15**, 85–93.
- Velde, B. (1984) Electron microprobe analysis of clay minerals. *Clay Minerals*, **19**, 243–247.
- Walker, G.G. (1961) Vermiculite minerals. Pp. 297–324 in: *The X-ray Identification and Crystal Structures of Clay Minerals* (G.W. Brindley and G. Brown, editors). Mineralogical Society, London.
- Warren, E.A. and Ransom, B. (1992) The influence of analytical error upon the interpretation of chemical variations in clay minerals. *Clay Minerals*, **27**, 193–209.
- Weaver, C.E. and Pollard, L.D. (1973) *The Chemistry of Clay Minerals*. Pp. 55–77. Elsevier, Amsterdam. The Netherlands.

(Received 3 April 2003; revised 17 July 2003; Ms. 778; A.E. David A. Laird)